Shape-Controlled Synthesis of Single-Crystalline Palladium Nanocrystals

Wenxin Niu,[†,‡] Ling Zhang,[†,‡] and Guobao Xu*[,†]

[†]State Key Laboratory of Electroanalytical Chemistry, Changchun Institute of Applied Chemistry and [‡]Graduate University of the Chinese Academy of Sciences, Chinese Academy of Sciences, Changchun 130022, China

ARTICLE

ABSTRACT A versatile method for selectively synthesizing single-crystalline rhombic dodecahedral, cubic, and octahedral palladium nanocrystals, as well as their derivatives with varying degrees of edge- and corner-truncation, was reported for the first time. This is also the first report regarding the synthesis of rhombic dodecahedral palladium nanocrystals. All the nanocrystals were readily synthesized by a seed-mediated method with cetyltrimethylammonium bromide as surfactant, KI as additive, and ascorbic acid as reductant. At the same ascorbic acid concentration, a series of palladium nanocrystals with varying shapes were obtained through manipulation of the concentration of KI and the reaction temperature. The formation of different palladium facets were correlated with their growth conditions. In the absence of KI, the {100} palladium facets are favored. In the presence of KI, the concentration of KI and the reaction temperature play an important role on the formation of different palladium facets. The {110} palladium facets are favored at relatively high temperatures and medium KI concentrations. The {111} palladium facets are favored at relatively low temperatures and medium KI concentrations. The {100} palladium facets are favored at either very low or relatively high KI concentrations. These correlations were explained in terms of surface-energy and growth kinetics. These results provide a basis for gaining mechanistic insights into the growth of well-faceted metal nanostructures.

KEYWORDS: crystal growth · palladium · nanostructures · shape control · rhombic dodecahedron

Rational shape-controlled synthesis of metallic nanocrystals is of vital importance to understanding their growth mechanism and shape-dependent properties.[1−3] Over the past decade, significant progress has been made in the development of new synthetic methods for metal nanocrystals, and various nanostructures have been synthesized. Among these nanostructures, single-crystalline nanocrystals have received much attention. In principle, the shapes of single-crystalline face-centered-cubic (fcc) metal nanocrystals enclosed completely by equivalent {100}, {111}, and {110} facets are supposed to be cube, octahedron, and rhombic dodecahedron (RD), respectively.[4] Besides these three typical shapes, polyhedral single-crystalline fcc metal nanocrystals enclosed by two and three of the {100}, {111}, and {110} facets can also be predicted theoretically. The representative shapes of these nanocrystals are shown in Figure 1. Although thousands of papers reported the preparations of metal nanostructures with different shapes, it is still challenging to synthesize multiple shapes with only one method and correlate the experimental results with synthetic conditions.[2,3] Among different synthetic methods of metal nanostructures, the seed-mediated growth method has been proved to provide better control over the size and shape evolution of metal nanostructures.[1] In previous studies, we found that the adoption of single-crystalline seeds with relatively large sizes in seed-mediated growth method can avoid the structure fluctuations of the nanoparticles during the growth stage, and consequently lead to the formation exclusively of single-crystalline nanocrystals.[5,6] This "large seeds" strategy could enable us to study the detailed correlations between growth conditions and the shapes of the single-crystalline metal nanocrystals during the growth stage and subsequently gain more mechanistic insights into the growth of metal nanocrystals.

Palladium plays important roles in hydrogen storage, gas-sensing, and catalysis;[7−9] therefore, palladium nanostructures have received increasing attention in recent years.[6,10−20] In this study, we synthesized single-crystalline palladium nanocrystals with varying shapes by using the "large seeds" strategy. Through systematically studying the effect of experimental conditions on the shape evolution of palladium nanocrystals, single-crystalline rhombic dodecahedral, cubic, and octahedral palladium nanocrystals, as well as their derivatives with varying degrees of edge- and corner-truncation, were all obtained. We correlated the formation of different shapes

*Address correspondence to guobaoxu@ciac.jl.cn.

Received for review January 16, 2010 and accepted March 12, 2010.

Published online March 22, 2010.
10.1021/nn100093y

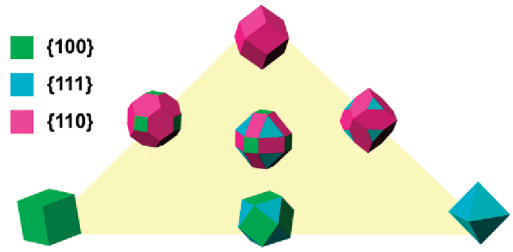

Figure 1. Geometrical models of several typical single-crystalline palladium nanocrystals enclosed by the {100}, {111}, and {110} facets. The {100}, {111}, and {110} facets are shown in green, blue, and purple, respectively.

of palladium nanocrystals with their corresponding growth conditions. The formation mechanisms for these nanocrystals were also discussed.

RESULTS AND DISCUSSION

Synthesis and Characterization of Single-Crystalline Palladium Nanocrystals. The seed-mediated growth method we used in this study is similar to the method in our previous report about the synthesis of palladium nanocubes.[6] Here we extended the versatility of this method to synthesize other single-crystalline palladium nanocrystals. First, small palladium nanocubes about 22 nm in size were synthesized through a one-step reduction and then employed as seeds for the seed-mediated growth procedure. The TEM image of these nanocubes is shown in Figure S1 in the Supporting Information. The 22 nm palladium nanocubes were subsequently grown into polyhedral nanocrystals in growth solutions containing cetyltrimethylammonium bromide (CTAB), dihydrogentetrachloropalladate(II) (H_2PdCl_4), potassium iodide (KI), and ascorbic acid (AA). Through manipulation of the concentration of KI and the reaction temperature, several types of palladium nanocrystals were synthesized. Figure 2 shows the palladium nanocrystals obtained with varying KI concentrations and reaction temperatures. In columns A−E, the reaction temperatures were 30, 40, 50, 60, and 80 °C, respectively. In rows 1−5, 5 μL of 100 mM, 5 μL of 10 mM, 25 μL of 1 mM, 5 μL of 1 mM, and 5 μL of 0.1 mM of KI solution were added to the growth solutions, respectively. In row 6, no KI was added to the growth solutions. In rows 1−5, the final KI concentrations in the reaction solution are 9.6×10^{-2}, 9.6×10^{-3}, 4.8×10^{-3}, 9.6×10^{-4}, and 9.6×10^{-5} mM, respectively. Figure 2 shows that a number of different shapes of palladium nanocrystals were observed besides the cubic palladium nanocrystals. For clarity, the corresponding geometrical models of these palladium nanocrystals in Figure 2 are presented in Figure 3. Cube, octahedron, and RD are three typical shapes of palladium nanocrystals enclosed completely by equivalent low-index palladium facets. All of them were obtained through this seed-mediated growth method in high yields (above 95%). Their structures were characterized through scanning electron microscope (SEM) and transmission electron microscope (TEM).

The SEM and TEM images of RD palladium nanocrystals (Sample E3 in Figure 2) are shown in Figure 4A,B. The geometrical shapes of these palladium nanocrystals can be clearly identified as perfect RD enclosed by 12 equivalent rhombic faces.[21] All the RD palladium nanocrystals have well-defined faces. Figure 4C shows the TEM image of a single flatly lying RD palladium nanocrystal. It exhibits an elongated hexagonal shape. Figure 4D shows a typical SAED pattern of a flatly lying RD palladium nanocrystals along the [011] zone axis obtained by directing the electron beam perpendicular to the upper face of the nanocrystal. These obserations are consistent with previous studies about RD gold nanocrystals,[22] proving that the RD palladium nanocrystals are enclosed by 12 well-defined {110} facets. Figure 4E and Supporting Information Figure S2B show the HRTEM image and its enlarged version of a RD palladium nanocrystal recorded along the [011] zone axis, respectively. The HRTEM image was taken at the RD nanocrystal in Supporting Information, Figure S2A. The continuous fringes and the fringe orientation in the HRTEM image confirm the morphology of single-crystalline RD palladium nanocrystals.[23]

Figure 5 shows the SEM and TEM characterizations of the cubic palladium nanocrystals (Sample D5 in Figure 2). These nanocubes have nearly perfect sharp edges and corners and well-defined faces. Figure 5C,D shows the TEM image and corresponding SAED pattern of a single palladium nanocube. The characteristic square spot array of the SAED pattern confirms that the palladium nanocubes are enclosed by well-defined {100} facets.[6,13] Figure 5E and S2D show the HRTEM image and its enlarged version of a cubic palladium nanocrystal recorded along the [001] zone axis, respectively. The HRTEM results agree well with previous reports about palladium nanocubes.[13,24]

SEM and TEM images of the octahedral palladium nanocrystals (Sample A3 in Figure 2) are presented in Figure 6. The SAED pattern of the octahedral palladium nanocrystals in Figure 6C,D is similar to that of previous reports about the single-crystalline octahedral gold nanocrystal enclosed by the {111} facets.[5,25] Figure 6E and Supporting Information, Figure S2F show the HRTEM image and its enlarged version of an octahedral palladium nanocrystal recorded along the [$\bar{1}$11] zone axis, respectively. The well-resolved, continuous lattice fringes with the same orientation confirm that the octahedral palladium nanocrystal is single-crystalline. Compared with the RD and cubic palladium nanocrystals with flat and smooth faces (Figures 4 and 5), the octahedral palladium nanocrystals have rough faces. In other samples of octahedral palladium nanocrystals (Sample A2, B3, and B4 in Figure 2), the faces

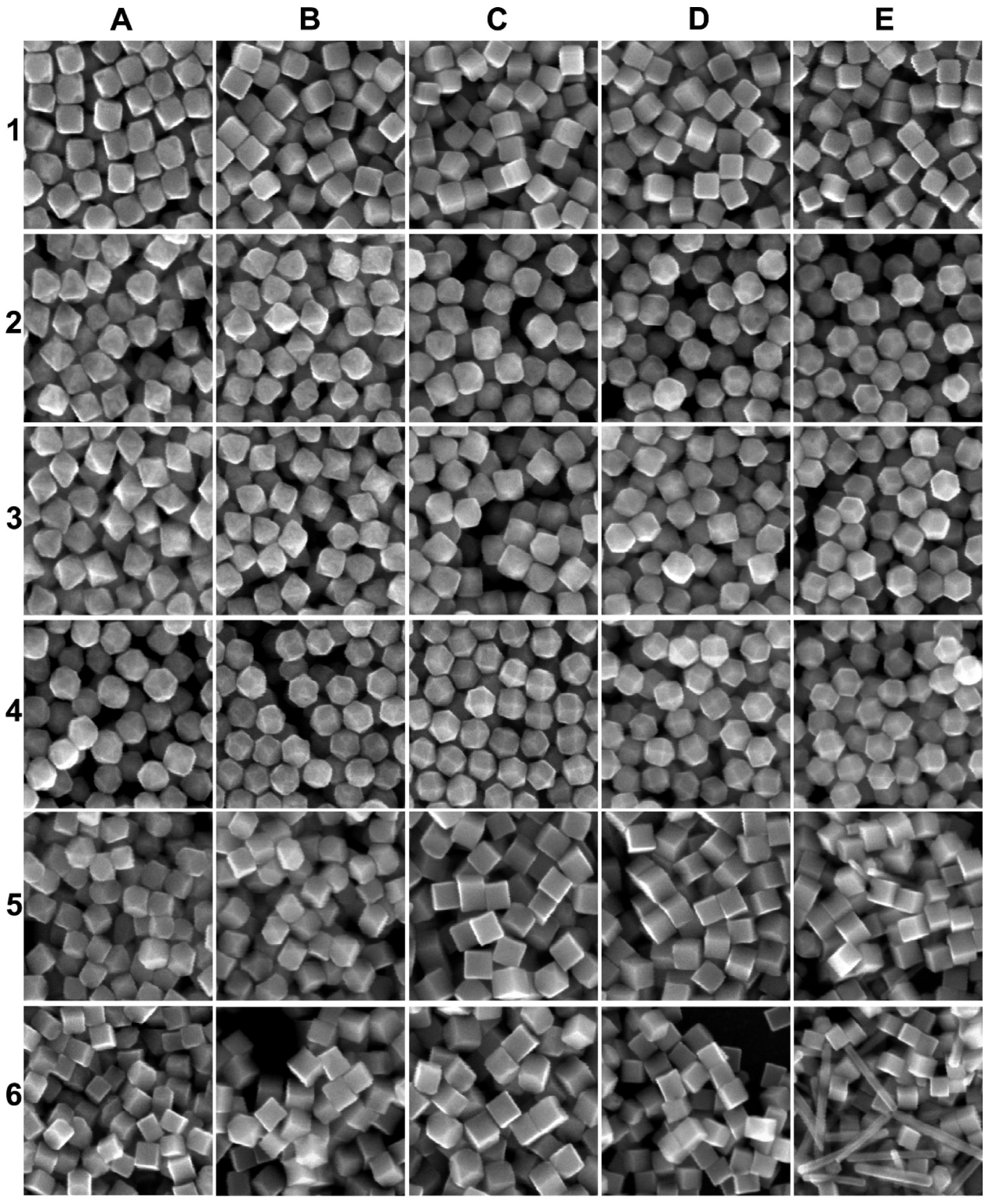

Figure 2. SEM images of polyhedral palladium nanocrystal samples synthesized under different conditions (scale bar: 200 nm). In columns A−E, the reaction temperatures are 30, 40, 50, 60, and 80 °C, respectively. In rows 1−5, 5 μL of 100 mM, 5 μL of 10 mM, 25 μL of 1 mM, 5 μL of 1 mM, and 5 μL of 0.1 mM KI solutions were added to the growth solutions, respectively. In row 6, no KI was added.

are even rougher. These rough faces suggest that the {111} facets are unstable under the synthetic conditions of these octahedral palladium nanocrystal.

The versatility of this method is not limited to the synthesis of the RD, cubic, and octahedral palladium nanocrystals. Figures 2 and 3 show that derivatives of the three typical shapes with varying degrees of

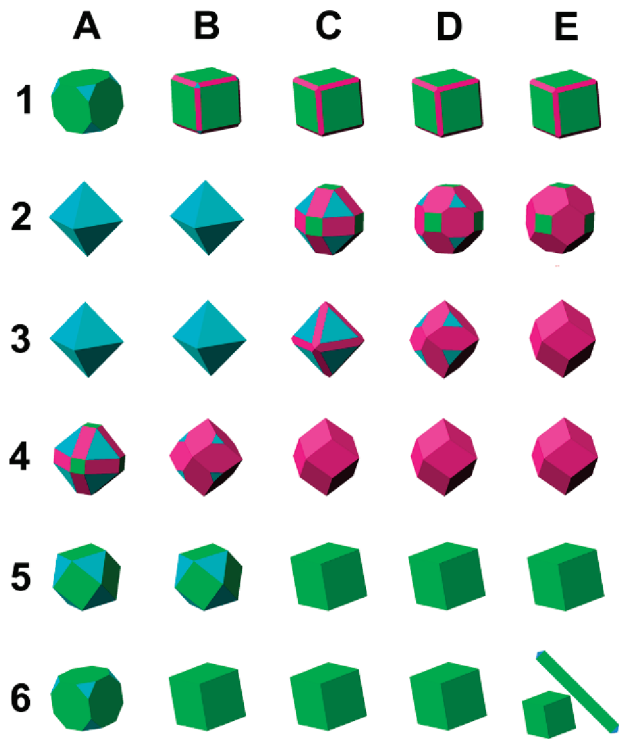

Figure 3. Geometrical models of palladium nanocrystals presented in Figure 2. The {100}, {111}, and {110} facets are shown in green, blue, and purple, respectively.

edge- and corner-truncation can also be obtained. These shapes can be easily identified on the basis of the three typical shapes. Samples B4 and D3 in Figure 2 consist of {111} truncated RD nanocrystals, while Sample E2 consists of {100} truncated RD nanocrystals. Sample D2 consists of both {100} and {111} truncated RD nanocrystals. Sample C3 consists of {110} truncated octahedral nanocrystals, while Samples A4 and C2 consist of both {110} and {110} truncated octahedral nanocrystals. Samples A1 and A6 consist of {111} truncated nanocubes. Samples A5 and B5 consist of cuboctahedral nanocrystals enclosed by six {100} facets and eight {111} facets. Sample B1 consists of both {110} and {111} truncated nanocubes. Samples C1, D1, and E1 consist of {110} truncated nanocubes. Sample E6 consists of both palladium nanorods and nanocubes.

On the basis of Figures 2 and 3, we can summarize the following correlations between the formation of palladium crystal facets and different growth conditions. In the absence of KI, the {100} palladium facets are favored. In the presence of KI, the concentration of KI and the reaction temperature play an important role on the formation of different palladium facets. The {110} palladium facets are favored at relatively high temperatures and medium KI concentrations. The {111} palladium facets are favored at relatively low temperatures and medium KI concentrations. The {100} palladium facets are favored at either very low or relatively high KI concentrations.

The X-ray diffraction (XRD) patterns recorded on the cubic, RD, and octahedral palladium nanocrystals are shown in Figure S3 in the Supporting Information. All of the peaks can be indexed to the fcc palladium metal (JCPDS Card no. 05-0681). The XRD pattern of palladium nanocubes shows an abnormally intense (200) peak, suggesting a relatively large proportion of the palladium nanocubes are oriented with their {100} facets parallel to the substrate. In contrast, the XRD patterns of RD and octahedral palladium nanocrystals do not show intense (220) or (111) diffraction. This is because most of the RD and octahedral palladium nanocrystals are randomly oriented (Figures 4A and 6A). Similar phenomena have also been reported by others. For example, the XRD patterns of palladium nanocubes and nanorods primarily enclosed by {100} facets do not show increased intensity for Pd(200) diffraction.[20,24] The XRD pattern of concave polyhedral Pd nanocrystals enclosed by both {111} and {110} facets does not show intense (220) diffraction, either.[26] These observations and our XRD results can all be attributed to the random orientation of the palladium nanostructures. The UV−vis extinction spectra of palladium nanocrystals are shown in Figure S4 in the Supporting Information. All the palladium nanocrystals have a broad peak located in the 400−500 nm wavelength region, suggesting that the optical properties of these polyhedral palladium nanocrystals are not strongly dependent on their shapes.

Growth Mechanisms of the Polyhedral Palladium Nanocrystals. ***The Seed-Mediated Growth Method for Palladium Nanostructures.*** A typical seed-mediated growth process involves the preparation of small metal nanoparticles and their subsequent growth in growth solutions.[1] The seed-mediated growth method has been used to synthesize palladium nanostructures in a few reports.[13,20] However, the palladium nanostructures obtained in these reports have relatively low yields. A key criterion for a successful seed-mediated growth method is the nanostructures obtained should have the same crystal structure and shape. To improve the yields of palladium nanocubes, we adopted 22 nm Pd nanocubes as seeds. Compared with smaller Pd nanoparticles of 3−4 nm, single-crystalline Pd nanocubes with such sizes are large enough to avoid twinning during the growth procedure, enabling us to correlate the shapes of the single-crystalline palladium nanocrystals with their growth conditions.[6] It has also been reported that non-palladium seeds, such as single-crystalline gold nanorods, platinum nanocubes, and gold nano-octahedra with relatively large sizes, can also avoid twinning during the deposition of palladium shells.[12,14,27]

Another key criterion for a successful seed-mediated growth method is whether spontaneous nucleation occurs during the growth procedure.[1] For the seed-mediated growth method, spontaneous nucleation means that the reduction of metal salts spontaneously

occurs in homogeneous solution without the surface catalysis of the added seeds. If the spontaneous nucleation occurs, it will lead to the formation of smaller nuclei and the formation of nanostructures with different sizes and structures. In our method, three factors play important roles on spontaneous nucleation. The first factor is the amount of seeds added to the growth solution. If too few seeds are added to the growth solution, spontaneous nucleation will occur because there are too few deposition spots.[6] The second factor is the reaction temperature. The generation rate of palladium atoms is accelerated at high temperatures. A certain amount of seeds cannot provide enough deposition spots for palladium atoms at a high generation rate, so spontaneous nucleation will occur. Sample D6, C6, B6, and A6 in Figure 2 show that spontaneous nucleation was avoided below 60 °C. When the temperature was raised to 80 °C, spontaneous nucleation occurred and led to the formation of 5-fold-twinned palladium nanorods (Sample E6 in Figure 2). The 5-fold-twinned palladium nanorods are primarily enclosed by {100} surfaces and have been observed in other reports using CTAB as surfactant.[11,19] The third factor is KI. The addition of KI can depress spontaneous nucleation. Sample E6 in Figure 2 shows that spontaneous nucleation occurred in the absence of KI, in contrast, spontaneous nucleation was not obvious when KI solutions were added (Sample E1−4 in Figure 2). These results demonstrate that KI can improve the preference of catalytic deposition of palladium atoms on the preformed seeds and thus depress spontaneous nucleation.

In the growth stage of the seed-mediated growth method, both thermodynamic and kinetic factors should have been taken into consideration to understand the formation mechanism of palladium nanocrystals.[1−3] If thermodynamic factors dominate, the shapes of nanocrystals will form as a result of surface energy minimization. If kinetics dominates, the shapes of nanocrystals are determined by the rate at which different crystal faces grow. In realistic solution reactions, the final state of the nanocrystals depends on these two factors working synergistically and dynamically. So it is extremely difficult to strictly determine the influence of each parameter on one specific shape of nanocrystals. In the following part, we will discuss the growth mechanism by comparing the surface energies of different facets and the preferential reduction of palladium salts on different facets.

The Formation of Cubic Palladium Nanocrystals in the Absence of KI or in the Presence of Low Concentrations of KI. As shown in Figure 3, the {100} palladium facets are favored in the absence of KI or in the presence of low concentrations of KI (with only 5 μL of 0.1 mM KI solutions added). Palladium nanostructures enclosed by {100} facets were commonly observed in previous reports that used CTAB as surfatants.[6,13−16,19] Bromide anions from the CTAB are believed to adsorb to the surface of palladium nanoparticles and promote to the formation of the {100} facets. CTAB plays a similar role herein. On the other hand, two reports show that palladium nanocrystals bearing {111} facets can also be obtained in the presence of CTAB.[6,13] The truncated cubic nanocrystals in Sample A6 of Figure 2 also have eight small {111} facets, suggesting CTAB can also stabilize the {111} facets of palladium. In the presence of CTAB, the {111} palladium facets were not commonly observed, suggesting it is not as stable as the palladium {100} facets. As the {110} facets are not observed in the presence of CTAB, the palladium {110} facets should be the most unstable low-index facet in the presence of CTAB. Therefore, CTAB can alter the surface energies of palladium facets in the order $\gamma_{\{100\}} < \gamma_{\{111\}} < \gamma_{\{110\}}$ in our synthetic conditions.

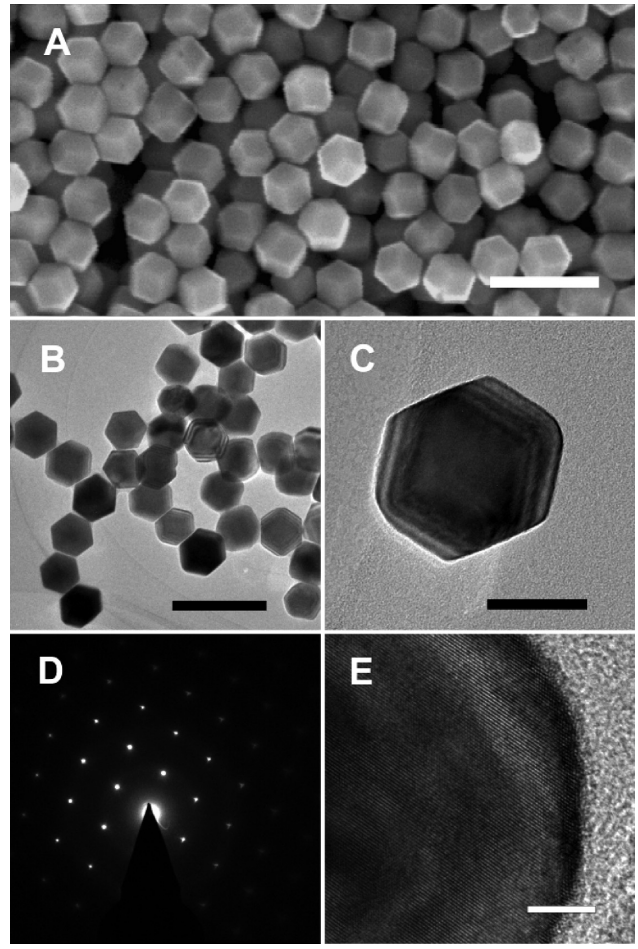

Figure 4. (A) SEM and (B) TEM images of RD palladium nanocrystals (scale bars, 200 nm); (C) TEM image and (D) corresponding SAED pattern of a single RD palladium nanocrystal recorded along the [011] zone axis (scale bar, 50 nm); (E) HRTEM image of a RD palladium nanocrystal (scale bar, 5 nm).

The surface energies of palladium facets and the final growth results cannot be significantly changed when KI was present in the growth solutions at very low concentrations. Samples A5 and B5 in Figure 2 were synthesized with the addition of only 5 μL of 0.1 mM KI solution, while Samples A6 and B6 were synthesized in the absence of KI. By comparison, we

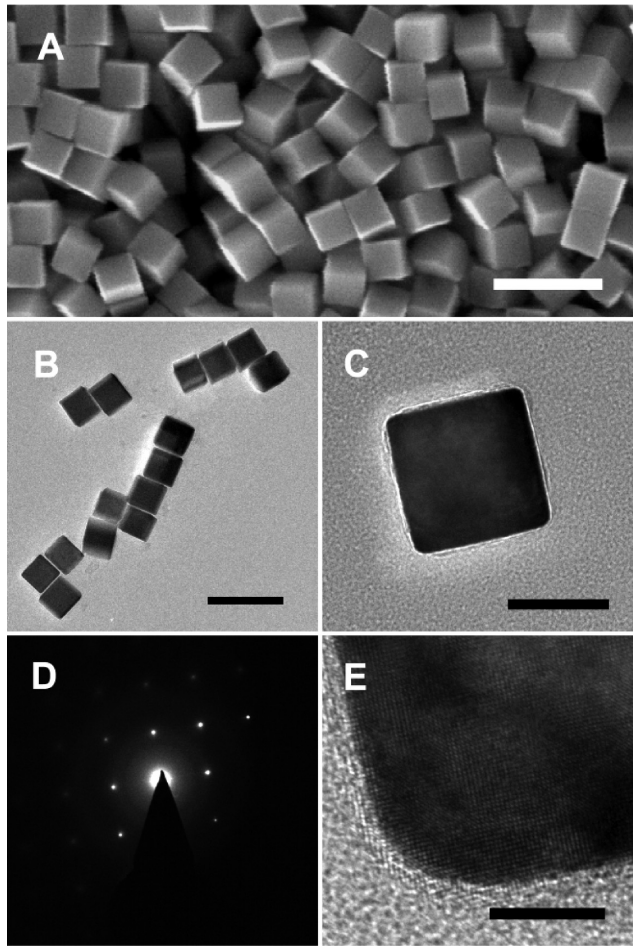

Figure 5. (A) SEM and (B) TEM images of cubic palladium nanocrystals (scale bars, 200 nm); (C) TEM image and (D) corresponding SAED pattern of a single cubic palladium nanocrystal recorded along the [001] zone axis (scale bar, 50 nm); (E) HRTEM image of a cubic palladium nanocrystal (scale bar, 5 nm).

found that the {111} facets became a little bit larger and the {100} facets became a little bit smaller when KI was introduced. These results suggest that KI can change the ratio between the growth rates along ⟨100⟩ and ⟨111⟩ directions. Generally, two possible explanations have been used to explain the change of the ratio between the growth rates along different directions: the selective accelerated growth or passivation of a special facet. In the present growth condition, the addition of 5 μL of 0.1 mM KI solution results in a quicker color change of the reaction solution and faster precipitation of the resulting nanocrystals, suggesting the overall reaction rate was accelerated. The accelerated growth of a special facet should be the reason for the change of growth rates of different facets. Consequently, we propose that KI can accelerate the deposition of palladium atoms on the {100} facets and thus reduce the areas of the {100} facets and enlarge the areas of the {111} facets.

In a realistic reaction, changes in the growth kinetics can lead to the formation of thermodynamically less-favored crystal facets.[3] Control experiments in Figure 7A,B show that cuboctahedral palladium nanocrystals enclosed by both the {100} and {111} palladium facets were produced at relatively low AA concentrations, while cubic nanocrystals enclosed completely by the {100} facets were produced at relatively high AA concentrations. These results suggest that the reduction of palladium salts to palladium atoms prefers to occur on the {111} facets under the present growth condition. Therefore, the growth of palladium nanocubes is attributed to the preferential reduction of palladium salts on the {111} facets, leading to the disappearance of the {111} facets and the formation of the {100} facets. When the preferential reduction on the {111} facets was slowed down by decreasing the concentration of AA, the {111} facets can also appear and thus truncated nanocubes were formed (Figure 7A).

The cuboctahedral and truncated cubic palladium nanocrystals were both obtained at relatively low temperatures such as 30 and 40 °C (Samples A5, A6, and B5 in Figure 2). When the temperature was raised to 50, 60, or 80 °C, the {111} facets disappeared and the {100} facets became dominant. These results suggest that relatively high temperatures promote the preferential reduction of palladium salts on the {111} facets, therefore the {111} facets vanished at relatively high temperatures.

Formation of RD and Octahedral Palladium Nanocrystals at Medium KI Concentrations. ***The Role of KI on the Growth of Palladium Nanocrystals.*** The adsorption of halide anions onto noble metal surfaces has a dramatic impact on the shape evolution of metal nanocrystals.[3,28] Iodide anions can greatly affect the shapes of gold nanocrystals.[28−30] Recently iodide anions have also been used to control the shapes of palladium nanostructures. Xiong and co-workers have studied the chemisorption of iodide on the palladium nanocrystal surface in growth solutions containing poly(vinylpyrrolidone) (PVP), water, and ethylene glycol.[31] They have found that the chemisorption of iodide on the nanocrystal surface is too strong for palladium nanoparticles to grow into larger sizes with a well-defined shape. Huang and co-workers have reported the preparation of palladium nanorods by the reduction of palladium(II) chloride with PVP in the presence of NaI under hydrothermal condition.[17] They have also reported the preparation of palladium nanocubes by the reduction of palladium acetylacetonate in the presence of PVP and NaI in mixed water/DMF solvent under hydrothermal condition.[18] In these studies, iodide anions have different effects on the growth results, due to different reaction media, precursors, and growth kinetics.

Surface energies associated with different face-centered cubic metal facets usually increase in the order $\gamma_{\{111\}} < \gamma_{\{100\}} < \gamma_{\{110\}}$.[23,26] For synthesis in solution phase, adsorbates such as surfactants and halide can interact selectively with different metal crystal facets and

alter their surface energies.[3] In this study, the addition of adequate KI can also alter the surface energies of different palladium facets by adsorbing to their surfaces. Previous reports show that the strength of chemisorption of halide on different palladium facets decreases in the order of iodide > bromide > chloride, and when a heavier halide is introduced into the solution, it will displace the lighter one initially present on the palladium surface.[32,33] Therefore, when KI was introduced in the growth solution, the iodide anions could replace some of the bromide anions on the surface of palladium nanocrystals and the selective interaction of iodide and different palladium facets alters the surface energies of palladium. As shown in Figures 4 and 5, both the {110} and {100} palladium facets are well-defined in the presence of CTAB and KI. In contrast, the {111} facets on the octahedral palladium nanocrystals are ill-defined in the presence of CTAB and KI (Figure 6). Therefore, we suppose that the {111} palladium facet is the most unstable facet of the three low-index facets in the presence of CTAB and a medium concentration of KI. The {110} palladium facets are only observed when KI was added in the CTAB solutions, suggesting the stability of the {110} palladium facets are greatly improved with the introduction of KI. Besides, the {110} palladium facets are more commonly observed than the {100} palladium facets at medium KI concentrations, therefore, the {110} facets are supposed to be more stable than the {100} facets. On the bais of these observations, it is reasonable to assume that the surface energy orders of the palladium low-index facets in the presence of CTAB and KI are $\gamma_{\{110\}} < \gamma_{\{100\}} < \gamma_{\{111\}}$.

Formation of RD and Octahedral Palladium Nanocrystals. Octahedral palladium nanocrystals were produced at relatively low temperatures and medium KI concentrations (Sample A3 in Figure 2). We believe that this is a kinetically controlled process, since the palladium {111} facets have the highest surface energy in the presence of CTAB and KI. Therefore, the octahedral palladium nanocrystals enclosed by {111} facets are not considered as thermodynamically favored shapes. We have conducted control experiments to understand the formation mechanism of the octahedral palladium nanocrystals through examining the effect of concentration of AA. Figure 7 panels C and D show the SEM images of palladium nanocrystals synthesized at two different AA concentrations while other conditions were the same as those in the synthesis of the octahedral palladium nanocrystals in Sample A3 in Figure 2. When the volume of 100 mM AA solution was decreased from 25 to 15 μL, the products changed from octahedral nanocrystals to polyhedral nanocrystals enclosed by {111}, {100}, and {110} facets. These observations suggest that the preferential growth of palladium atoms on the {110} and {100} facets are favored at relatively high AA concentrations (with 25 or 50 μL of 100 mM AA solution added), and thus lead to the disappearance of the {110} and {100} facets and the formation of octahedral nanocrystals. The rough nature of the octahedral palladium nanocrystals (Figure 6) should be attributed to the low stability and high surface energy of the {111} facets in the presence of CTAB and KI, and thus the {111} facets became rough as a result of surface reconstruction.

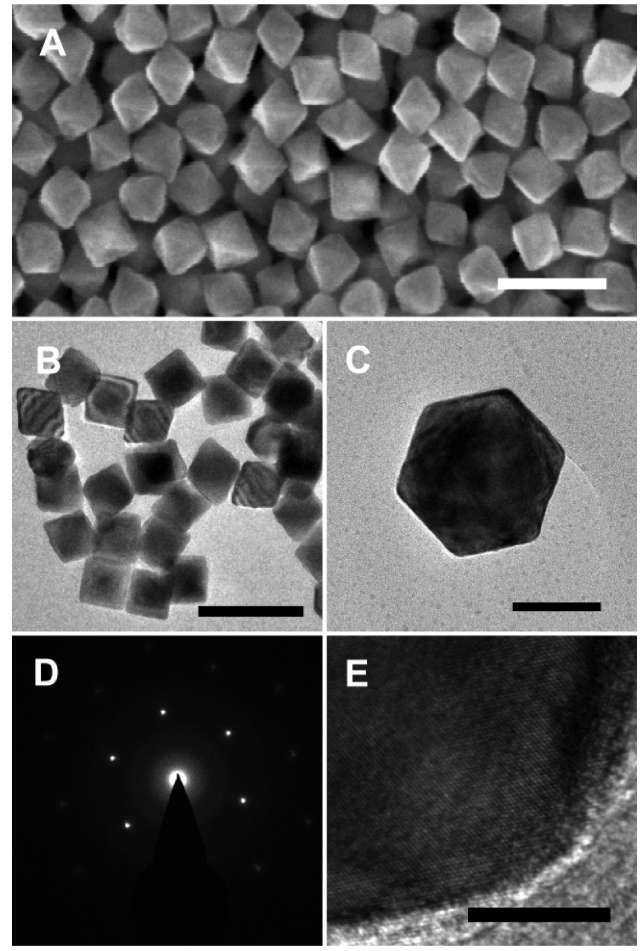

Figure 6. (A) SEM and (B) TEM images of octahedral palladium nanocrystals (scale bars, 200 nm); (C) TEM image and (D) corresponding SAED pattern of a single octahedral palladium nanocrystal recorded along the [$\bar{1}$11] zone axis (scale bar, 50 nm). (E) HRTEM image of an octahedral palladium nanocrystal (scale bar, 5 nm).

Compared with octahedral palladium nanocrystals, RD palladium nanocrystals were produced at relatively high temperatures (Sample E3 in Figure 2). Three aspects were taken into consideration to understand the formation mechanism of the RD palladium nanocrystals. (i) The addition of KI to CTAB solutions can significantly increase the stability of the palladium {110} facets. (ii) A relatively high temperature promotes the preferential reduction of palladium salts on the {111} facets. Consequently, the {111} palladium facets have a tendency to disappear at relatively high temperatures. (iii) A suitable AA concentration is also essential for the formation of RD palladium nanocrystals. Figure 7 panels E and F show the SEM images of palladium nanocrystals synthesized at different AA concentrations, all the other conditions are the same as those for Sample E3

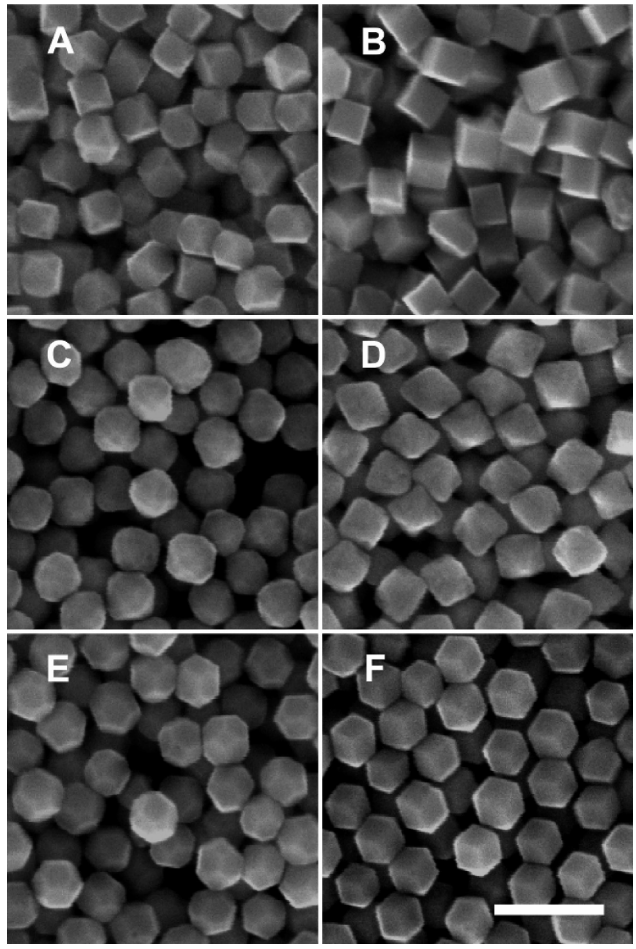

Figure 7. SEM images of palladium nanocrystals synthesized at different temperatures with the addition of different amounts of KI and AA (scale bar, 200 nm): (A) 30 °C, 5 μL of 0.1 mM KI solution, and 25 μL of 100 mM AA solution; (B) 30 °C, 5 μL of 0.1 mM KI solution, and 100 μL of 100 mM AA solution; (C) 30 °C, 25 μL of 1 mM KI solution, and 15 μL of 100 mM AA solution; (D) 30 °C, 25 μL of 1 mM KI solution, and 25 μL of 100 mM AA solution; (E) 80 °C, 25 μL of 1 mM KI solution, and 25 μL of 100 mM AA solution; (F) 80 °C, 25 μL of 1 mM KI solution, and 100 μL of 100 mM AA solution.

in Figure 2. Figure 7E shows that {100} truncated RD nanocrystals were obtained when 25 μL of 100 mM AA was added to the growth solutions. Figure 7F shows that perfect RD nanocrystals were obtained when 100 μL of 100 mM AA was added. The formation of {100} facets at low AA concentrations suggests that the reduction of palladium salts to palladium atoms prefers to occur on the {100} facets, and thus the {100} facets will disappear if the preferential reduction on the {100} facets is promoted by adding more AA (50 or 100 μL). In summary, the formation of RD palladium nanocrystals should be attributed to the high stability of the {110} facets and the disappearance of both the {111} and {100} facets at the growth conditions of RD palladium nanocrystals.

Formation of Cubic Palladium Nanocrystals at Relatively High KI Concentrations. When 5 μL of 100 mM KI solution was added in the growth solutions, truncated palladium nanocubes were produced (Samples A1, B1, C1, D1, and E1 in Figure 2). The palladium {100} facets are predominant on these truncated nanocubes. After the addition of 5 μL of 100 mM KI solution, we did not observe the characteristic UV−vis adsorption peaks of the $[PdBr_{4-n}I_n]^{2-}$ complex (Supporting Information, Figure S5).[34] The adsorption peaks are ascribed to $PdBr_4^{2-}$,[13] suggesting $PdBr_4^{2-}$ is still the major precursor for palladium nanocrystals at relatively high KI concentrations (5 μL of 100 mM KI solution added). On the other hand, we observed that the color change of the above reaction solution is much slower, and the overall reaction speed was greatly slowed down, suggesting the excessive adsorption of iodide anions can passivate the palladium surfaces and slow down the deposition of palladium atoms. The excessive adsorption of iodide anions over all the three types of facets greatly weakened the preferential formation of a certain palladium facet, and thus the selectivity of iodide anions on the formation of palladium nanocrystals with special shapes was counteracted.[31] In this situation, the role of CTAB on the formation of palladium nanocrystals primarily enclosed by {100} facets became dominant and led to the formation of truncated palladium nanocubes.

CONCLUSION

We developed a versatile seed-mediated method to selectively synthesize single-crystalline rhombic dodecahedral, cubic, and octahedral palladium nanocrystals, as well as their derivatives with varying degrees of edge- and corner-truncation. This is the first report regarding the synthesis of rhombic dodecahedral palladium nanocrystals. All the nanocrystals were synthesized simply by varying the concentration of KI and reaction temperature. The formation of different palladium facets were correlated with the growth conditions. The correlations were explained in terms of surface-energy and growth kinetics. These results are helpful for gaining mechanistic insights into the growth of well-faceted metal nanostructures.

METHODS

Materials. Palladium(II) chloride ($PdCl_2$) and potassium iodide (KI) were obtained from Sinopharm Chemical Reagent Co., Ltd. CTAB was obtained from Fluka. L-Ascorbic acid and hydrochloric acid were obtained from Beijing Chemical Reagent Company. All the chemicals were of analytical grade and used without further purification. Doubly distilled water was used throughout the experiments. A 10 mM H_2PdCl_4 solution was prepared by dissolving 0.1773 g of $PdCl_2$ in 10 mL of 0.2 M HCl solution and further diluting to 100 mL with doubly distilled water.

Synthesis of Small Palladium Nanocubes as Seeds. In a typical synthesis, a 1 mL aliquot of 10 mM H_2PdCl_4 solution was added to 20 mL of 12.5 mM CTAB solution heated at 95 °C under stirring. After 5 min, 160 μL of freshly prepared 100 mM ascorbic acid solution was added, and the reaction was allowed to proceed for 20 min. The nanocube solution was stored at 30 °C for future use as seeds.

Seed-Mediated Growth of Polyhedral Palladium Nanocrystals. In a typical synthesis, a given amount of KI solutions were added to 5 mL of 100 mM CTAB solution kept at a given temperature. A 125 μL portion of 10 mM H_2PdCl_4 solution and 40 μL of the as-synthesized seed palladium nanocubes solution were then added. Finally, 50 μL of freshly prepared 100 mM ascorbic acid solution was added, and the solution was mixed thoroughly. The resulting solution was placed in a water bath at designated temperatures. Reactions at the same temperature were set up in parallel. The reaction time for reactions at 30, 40, 50, 60, and 80 °C were approximately 40, 15, 6, 2, and 1 h, respectively. The reactions were stopped by centrifugation (6000 rpm, 10 min). The precipitates were redispersed in doubly distilled water for UV−vis extinction spectra characterization. Two more centrifugations (6000 rpm, 10 min) were applied to the samples for scanning electron microscopy (SEM), transmission electron microscope (TEM), and XRD characterization.

Instrumentation. SEM images were taken using an FEI XL30 ESEM FEG scanning electron microscope operated at 25 kV. TEM and selected area electron diffraction (SAED) studies were performed on a FEI Tecnai G^2 20 S-TWIN TEM operated at 200 KV. UV−vis extinction spectra were taken at room temperature on a CARY 500 Scan UV−vis-near IR spectrophotometer using a quartz cuvette with an optical path of 1 cm. XRD samples were prepared by evaporating a drop of nanocrystal solution onto a glass substrate. XRD data were collected using Bruker D8 ADVANCE X-ray diffractometer (Cu Kα radiation) operated at 40 kV and 40 mA over a range of 30−90° by step scanning with a step size of 0.048° at room temperature.

Acknowledgment. We gratefully acknowledge support from the National Natural Science Foundation of China (Grants 20505016 and 20875086), the Ministry of Science and technology of the People's Republic of China (Grant 2006BAE03B08), and the Department of Sciences & Technology of Jilin Province (Grants 20070108 and 20082104).

Supporting Information Available: Figure S1−S5. This material is available free of charge *via* the Internet at http://pubs.acs.org.

REFERENCES AND NOTES

1. Murphy, C. J.; Sau, T. K.; Gole, A. M.; Orendorff, C. J.; Gao, J.; Gou, L.; Hunyadi, S. E.; Li, T. Anisotropic Metal Nanoparticles: Synthesis, Assembly, and Optical Applications. *J. Phys. Chem. B* **2005**, *109*, 13857–13870.
2. Tao, A. R.; Habas, S.; Yang, P. Shape Control of Colloidal Metal Nanocrystals. *Small* **2008**, *4*, 310–325.
3. Xia, Y.; Xiong, Y.; Lim, B.; Skrabalak, S. E. Shape-Controlled Synthesis of Metal Nanocrystals: Simple Chemistry Meets Complex Physics. *Angew. Chem., Int. Ed.* **2009**, *48*, 60–103.
4. Francis, C. A. Gold Crystals: A Primer. *Rocks Miner.* **2004**, *79*, 24–29.
5. Niu, W.; Zheng, S.; Wang, D.; Liu, X.; Li, H.; Han, S.; Chen, J.; Tang, Z.; Xu, G. Selective Synthesis of Single-Crystalline Rhombic Dodecahedral, Octahedral, and Cubic Gold Nanocrystals. *J. Am. Chem. Soc.* **2009**, *131*, 697–703.
6. Niu, W.; Li, Z.-Y.; Shi, L.; Liu, X.; Li, H.; Han, S.; Chen, J.; Xu, G. Seed-Mediated Growth of Nearly Monodisperse Palladium Nanocubes with Controllable Sizes. *Cryst. Growth Des.* **2008**, *8*, 4440–4444.
7. Jewell, L. L.; Davis, B. H. Review of Absorption and Adsorption in the Hydrogen−Palladium System. *Appl. Catal., A* **2006**, *310*, 1–15.
8. Favier, F.; Walter, E. C.; Zach, M. P.; Benter, T.; Penner, R. M. Hydrogen Sensors and Switches from Electrodeposited Palladium Mesowire Arrays. *Science* **2001**, *293*, 2227–2231.
9. Astruc, D. Palladium Nanoparticles as Efficient Green Homogeneous and Heterogeneous Carbon−Carbon Coupling Precatalysts: A Unifying View. *Inorg. Chem.* **2007**, *46*, 1884–1894.
10. Xiong, Y.; Xia, Y. Shape-Controlled Synthesis of Metal Nanostructures: The Case of Palladium. *Adv. Mater.* **2007**, *19*, 3385–3391.
11. Lim, B.; Jiang, M.; Tao, J.; Camargo, P. H. C.; Zhu, Y.; Xia, Y. Shape-Controlled Synthesis of Pd Nanocrystals in Aqueous Solutions. *Adv. Funct. Mater.* **2009**, *19*, 189–200.
12. Xiang, Y.; Wu, X.; Liu, D.; Jiang, X.; Chu, W.; Li, Z.; Ma, Y.; Zhou, W.; Xie, S. Formation of Rectangularly Shaped Pd/Au Bimetallic Nanorods: Evidence for Competing Growth of the Pd Shell between the {110} and {100} Side Facets of Au Nanorods. *Nano Lett.* **2006**, *6*, 2290–2294.
13. Berhault, G.; Bausach, M.; Bisson, L.; Becerra, L.; Thomazeau, C.; Uzio, D. Seed-Mediated Synthesis of Pd Nanocrystals: Factors Influencing a Kinetic- or Thermodynamic-Controlled Growth Regime. *J. Phys. Chem. C* **2007**, *111*, 5915–5925.
14. Habas, S. E.; Lee, H.; Radmilovic, V.; Somorjai, G. A.; Yang, P. Shaping Binary Metal Nanocrystals through Epitaxial Seeded Growth. *Nat. Mater.* **2007**, *6*, 692–697.
15. Chang, G.; Oyata, M.; Hirao, K. Facile Synthesis of Monodisperse Palladium Nanocubes and the Characteristics of Self-Assembly. *Acta Mater.* **2007**, *55*, 3453–3456.
16. Sun, Y.; Zhang, L.; Zhou, H.; Zhu, Y.; Sutter, E.; Ji, Y.; Rafailovich, M. H.; Sokolov, J. C. Seedless and Templateless Synthesis of Rectangular Palladium Nanoparticles. *Chem. Mater.* **2007**, *19*, 2065–2070.
17. Huang, X.; Zheng, N. One-Pot, High-Yield Synthesis of 5-Fold Twinned Pd Nanowires and Nanorods. *J. Am. Chem. Soc.* **2009**, *131*, 4602–4603.
18. Huang, X.; Zhang, H.; Guo, C.; Zhou, Z.; Zheng, N. Simplifying the Creation of Hollow Metallic Nanostructures: One-Pot Synthesis of Hollow Palladium/Platinum Single-Crystalline Nanocubes. *Angew. Chem., Int. Ed.* **2009**, *48*, 4808–4812.
19. Fan, F.-R.; Attia, A.; Sur, K. U.; Chen, J.-B.; Xie, Z.-X.; Li, J.-F.; Ren, B.; Tian, Z.-Q. An Effective Strategy for Room-Temperature Synthesis of Single-Crystalline Palladium Nanocubes and Nanodendrites in Aqueous Solution. *Cryst. Growth Des.* **2009**, *9*, 2335–2340.
20. Chen, Y.-H.; Hung, H.-H.; Huang, M. H. Seed-Mediated Synthesis of Palladium Nanorods and Branched Nanocrystals and Their Use as Recyclable Suzuki Coupling Reaction Catalysts. *J. Am. Chem. Soc.* **2009**, *131*, 9114–9121.
21. Weisstein, E. W. In *CRC Concise Encyclopedia of Mathematics*, 2nd ed.; CRC Press: Boca Raton, FL, 2003; p 2546.
22. Jeong, G. H.; Kim, M.; Lee, Y. W.; Choi, W.; Oh, W. T.; Park, Q.-H.; Han, S. W. Polyhedral Au Nanocrystals Exclusively Bound by {110} Facets: The Rhombic Dodecahedron. *J. Am. Chem. Soc.* **2009**, *131*, 1672–1673.
23. Wang, Z. L. Transmission Electron Microscopy of Shape-Controlled Nanocrystals and Their Assemblies. *J. Phys. Chem. B* **2000**, *104*, 1153–1175.
24. Xiong, Y.; Chen, J.; Wiley, B.; Xia, Y.; Yin, Y.; Li, Z.-Y. Size-Dependence of Surface Plasmon Resonance and Oxidation for Pd Nanocubes Synthesized *via* a Seed Etching Process. *Nano Lett.* **2005**, *5*, 1237–1242.
25. Seo, D.; Park, J. C.; Song, H. Polyhedral Gold Nanocrystals with O_h Symmetry: From Octahedra to Cubes. *J. Am. Chem. Soc.* **2006**, *128*, 14863–14870.
26. Huang, X.; Tang, S.; Zhang, H.; Zhou, Z.; Zheng, N. Controlled Formation of Concave Tetrahedral/Trigonal Bipyramidal Palladium Nanocrystals. *J. Am. Chem. Soc.* **2009**, *131*, 13916–13917.
27. Fan, F. R.; Liu, D. Y.; Wu, Y. F.; Duan, S.; Xie, Z. X.; Jiang, Z. Y.; Tian, Z. Q. Epitaxial Growth of Heterogeneous Metal Nanocrystals: From Gold Nano-octahedra to Palladium and Silver Nanocubes. *J. Am. Chem. Soc.* **2008**, *130*, 6949–6950.
28. Ha, T. H.; Koo, H. J.; Chung, B. H. Shape-Controlled Syntheses of Gold Nanoprisms and Nanorods Influenced by Specific Adsorption of Halide Ions. *J. Phys. Chem. C* **2007**, *111*, 1123–1130.
29. Millstone, J. E.; Wei, W.; Jones, M. R.; Yoo, H.; Mirkin, C. A. Iodide Ions Control Seed-Mediated Growth of Anisotropic Gold Nanoparticles. *Nano Lett.* **2008**, *8*, 2526–2529.

30. Smith, D. K.; Miller, N. R.; Korgel, B. A. Iodide in CTAB Prevents Gold Nanorod Formation. *Langmuir* **2009**, *25*, 9518–9524.
31. Xiong, Y.; Cai, H.; Wiley, B. J.; Wang, J.; Kim, M. J.; Xia, Y. Synthesis and Mechanistic Study of Palladium Nanobars and Nanorods. *J. Am. Chem. Soc.* **2007**, *129*, 3665–3675.
32. Carrasquillo, A.; Jeng, J.-J., Jr.; Barriga, R. J.; Temesghen, W. F.; Soriaga, M. P. Electrode-Surface Coordination Chemistry: Ligand Substitution and Competitive Coordination of Halides at Well-Defined Pd(100) and Pd(111) Single Crystals. *Inorg. Chim. Acta* **1997**, *255*, 249–254.
33. Wieckowski, A.; Itaya, K. In *Proceedings of the Sixth International Symposium on Electrode Processes*; The Electrochemical Society, Inc.: NJ, 1996; pp 58−67.
34. Srivastava, S. C.; Newman, L. Mixed-Ligand Complexes of Palladium(II) with Bromide and Iodide. *Inorg. Chem.* **1967**, *6*, 762–765.